Mechanisms of Ligand Recognition in Myoglobin

Barry A. Springer*

Department of Chemical and Physical Sciences, Crystallography and Biophysical Chemistry, The DuPont Merck Pharmaceutical Company, P.O. Box 80228, Wilmington, Delaware 19880-0228

Stephen G. Sligar*

Departments of Biochemistry and Chemistry, University of Illinois, Urbana, Illinois 61801

John S. Olson* and George N. Phillips, Jr.*

Department of Biochemistry and Cell Biology and W.M. Keck Center for Computational Biology, Rice University, Houston, Texas 77251

Received December 8, 1993 (Revised Manuscript Received February 18, 1994)

Contents

I. Introduction

The structural elements which afford molecular recognition and discrimination events in macromolecule–ligand interactions dictate the basis of protein function. Nature has evolved highly specific interactions between proteins and other molecules that permit regulated biological activities, without which life could not exist. Selected examples include enzyme–substrate, receptor–ligand, antibody–antigen, and protein–nucleic acid interactions. The mechanisms which allow the binding of one ligand preferentially over chemically and structurally similar molecules is defined at the atomic level. In this review we will focus on the ability of the heme proteins myoglobin and hemoglobin to discriminate selectively between the binding of two small gaseous ligands, oxygen (O_2) and carbon monoxide (CO). Although the chemical and structural rules which define this interaction are unique to myoglobin and hemoglobin, the underlying mechanisms have general applicability to all protein–ligand interactions. As will become apparent to readers, the combination of site-directed mutagenesis to modify specifically a protein active site, coupled with structural, chemical, and physical characterizations of the resultant mutant proteins, provides a very powerful approach from which to address protein function at the molecular level. Only when knowledge of proteins at this level is attained does the rational design of chemical and structural ligand analogs become possible.

Hemoglobin and myoglobin are partners in the transport and storage of oxygen in vertebrates. Hemoglobin is found packed at high concentrations (~20 mM) in red blood cells and myoglobin in aerobic muscle tissue. Hemoglobin is an $\alpha_2\beta_2$ heterotetramer that binds O_2 cooperatively. The cooperative binding of O_2 in areas of high oxygen concentration allows hemoglobin to become nearly saturated in the lungs. The blood stream then transports oxyhemoglobin to areas of low oxygen concentration in respiring tissues where the O_2 is released and delivered to myoglobin. Myoglobin is a compact, predominantly α-helical, globular protein which functions by storing oxygen during periods of rest until required for oxidative phosphorylation. The individual α and β subunits of hemoglobin are analogous to myoglobin both at the structural and functional levels. Although a brief comparison of the functional properties of myoglobin and the hemoglobin subunits will be addressed below, a complete description of hemoglobin structure and function is beyond the scope of this review and readers are directed to the following reviews for more extensive information.[1-4]

0009-2665/94/0794-0699$14.00/0

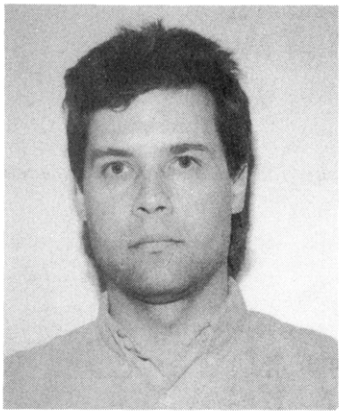

Barry A. Springer received a Ph.D. in Biochemistry from the University of Illinois, Urbana, Illinois, in 1989. Following postdoctoral work as a Helen Hay Whitney Fellow in the Chemistry department at the University of California, Berkeley, he moved to the Structural Biology department at DuPont Central Research and Development. Barry is currently a Senior Research Scientist in the Department of Chemical and Physical Sciences at the DuPont Merck Pharmaceutical Company. His current efforts are focused on characterization of macromolecular recognition events in protein–protein, protein–ligand, and protein–carbohydrate interactions.

Stephen Sligar received his Ph.D. in Physics from the University of Illinois in 1975. He is chair of the School of Chemical Sciences and a professor in the departments of Chemistry and Biochemistry at the University of Illinois at Urbana-Champaign and a part-time Beckman Institute faculty member in the Advanced Chemical Systems Group. Some of Prof. Sligar's awards and honors are as follows: Fellow, AAAS; Janet and William Lycan Endowed Chair; Fulbright Research Scholar, Institut de Biologie Physico-Chimique, Paris and Yale University (1989-1990); National Institutes of Health Research Career Development Awardee (1980-1985); Sigma Pi Sigma; Pi Mu Epsilon; Phi Kappa Phi; Sigma Xi; Alpha Chi Sigma. One facet of Prof. Sligar's research lies in the area of molecular recognition and involves examining the fundamental principals of protein–protein, protein–nucleic acid, and protein–small molecule interactions using a combination of site-directed mutagenesis, computer modeling, and structure determination. A second area of work is in biomolecular electronics. Here his work centers on the synthesis and physical characterization of highly ordered protein superlattices.

George N. Phillips, Jr., born in 1952, received his B.A. in Chemistry and Biochemistry (1974) and Ph.D. in Biochemistry (1977) from Rice University. After postdoctoral work at Brandeis University and five years as an Assistant Professor at the University of Illinois at Urbana–Champaign, he returned to Rice University where he is now Professor of Biochemistry and Cell Biology. Phillips's research begins with a solid understanding of the three-dimensional structures of important biological molecules and then moves on to study experimental and theoretical aspects of their dynamics to develop a better understanding of the mechanisms involved in the biological function of the systems.

John S. Olson was born in Evanston, IL, and received his B.S. in Chemistry from the University of Illinois, Champaign–Urbana in 1968 and his Ph.D. in Biochemistry from Cornell University in 1972 under the guidance of Quentin H. Gibson. He was an NIH postdoctoral fellow with Vincent Massey in the Department of Biological Chemistry at the University of Michigan, Ann Arbor, and then joined the faculty at Rice University in 1973 where he is currently a Professor of Biochemistry and Cell Biology. Olson's Laboratory has been using biochemical, biophysical, site-direct mutagenesis, and chemical engineering approaches to examine the fundamental processes involved in oxygen transport and storage in mammalian circulatory systems. The results are being applied to an understanding of the dynamics of ligand binding to myoglobins and hemoglobins, to predictions of mass transport in capillary systems, and to the design of heme protein-based blood substitutes.

Sperm whale myoglobin and horse hemoglobin A were the first protein structures determined to high resolution by X-ray crystallography[5,6] and have since served as paradigms for studies of protein structure–function correlation. Myoglobin is comprised of eight α helices (labeled A-H) that form an amphipathic pocket that stabilizes the binding of the essential prosthetic group, iron protoporphyrin IX, which is designated as heme (Fe^{2+}) or hemin (Fe^{3+}) (Figure 1). The iron atom is coordinated to the protein moiety through a histidine which is located at position 8 along the F helix (HisF8, or "proximal" histidine) (Figures 1 and 2) and to the protoporphyrin through four pyrrole nitrogens. The majority of the other heme–protein contacts are hydrophobic, with the exception of two solvent-exposed heme propionates that interact electrostatically with external protein residues.

Myoglobin and hemoglobin bind ligands through the one remaining Fe coordination position on the distal face of the heme. The heme iron in myoglobin and hemoglobin exists in two physiologically relevant ox-

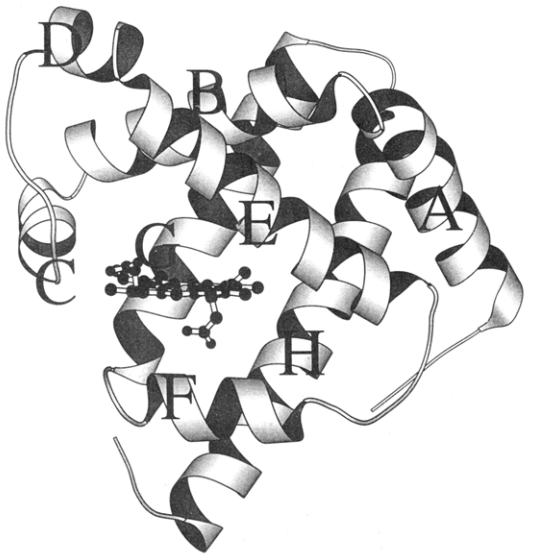

Figure 1. A ribbon diagram of the sperm whale myoglobin α-carbon backbone showing the arrangement of the eight α helices and the heme group (shown as balls and sticks).[115] To simplify the comparison to other oxygen binding heme proteins, the location of a particular amino acid is specified by a location along a helix, instead of the simple numerical value in the sequence. For example, amino acid E7 is the seventh amino acid along the E helix. Amino acids in turns between helices are specified by a number following the two helix specifiers, e.g., CD1. Figures 1–6 were prepared using MOLSCRIPT.[116]

idation states. In the oxidized (Fe^{3+}, ferric, or met) state, myoglobin and hemoglobin can bind a water molecule or a number of different anions (viz. N_3^-, CN^-, NO_2^-, SCN^-, and F^-). In the reduced (Fe^{2+}, ferrous, deoxy) state, myoglobin and hemoglobin can bind O_2, CO, NO, aryl nitroso compounds, and alkyl isocyanides.[7,8] In this review, our attention will be focused on O_2 and CO binding.

Unhindered pentacoordinate model hemes in organic solvents bind oxygen and carbon monoxide with a ratio that favors CO over O_2 by as much as 30 000- to 100 000-fold.[9–14] When the heme is embedded in the protein matrix of myoglobin or hemoglobin, that ratio is changed to approximately 30 and 200, respectively. Thus, these proteins are capable of selectively discriminating against the binding of carbon monoxide in favor of oxygen. This mechanism of preferential O_2 binding has evolved to prevent inhibition of oxygen transport and storage by endogenously produced carbon monoxide. Both the catabolic breakdown of heme and related neurotransmission activity produce sufficient CO to inhibit hemoglobin and myoglobin function if the proteins had the same relative O_2 and CO affinities as simple heme complexes.[15,16]

In order for myoglobin and hemoglobin to function as efficient oxygen transport and storage proteins, they must also have appropriate kinetic and thermodynamic properties with respect to oxygen binding. In hemoglobin, the affinity for oxygen must be moderately low (P_{50} of 20–50 μM) in order to release the oxygen when needed, and relatively large association and dissociation rate constants ($k'_{O_2} > 10^6$ M^{-1} s^{-1} and $k_{O_2} > 10$ s^{-1}) are required for rapid release and uptake in muscle and capillary beds.[17,18] The proteins must also be slow to autooxidize to the ferric state, have low rates of hemin dissociation, and be resistant to denaturation.

II. General Aspects of Heme Protein–Ligand Interactions

A. Proximal Coordination Geometry

The presence of a proximal base has a profound influence on the reactivity of the heme iron. In the absence of a fifth ligand, the equilibrium constant for CO binding is reduced several hundred-fold and reversible oxygen binding does not occur due to extremely rapid rates of autooxidation. The nature of the proximal base helps to determine the enzymatic activity of the heme protein with cysteine, tyrosine, and imidazole being found in P_{450} oxygenases, catalases, and peroxidases, respectively. In cytochrome *c* peroxidase, the proximal histidine forms a hydrogen bond with an adjacent ionized aspartic acid residue giving

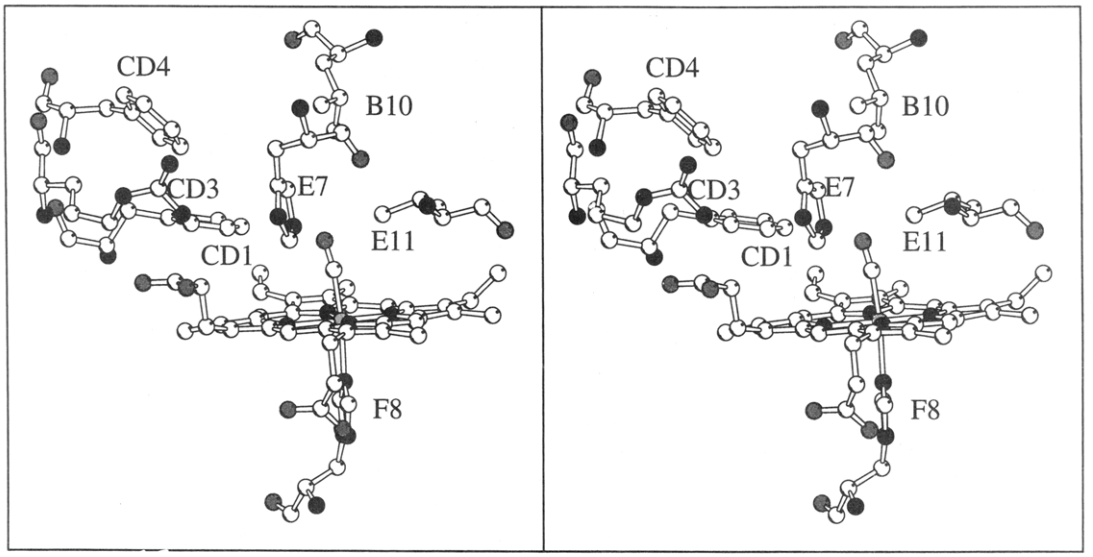

Figure 2. A stereoview of the heme with bound CO and arrangement of amino acids in the distal pocket (ligand binding site) of sperm whale myoglobin.[115] These key active site amino acids have been replaced by site-directed mutagenesis to examine their roles in O_2/CO discrimination. The proximal histidine (HisF8) coordinated to the heme iron is also shown. Carbon atoms are displayed as open circles, nitrogen atoms as closed circles, and oxygen atoms as shaded circles.

the imidazole side chain anionic character and facilitating the reduction of hydrogen peroxide.[19] In the oxygen transport proteins, the proximal imidazole is neutral and facilitates the reversible binding of oxygen and carbon monoxide.

Restraints on the proximal histidine bond can affect greatly the affinities of myoglobins and hemoglobins for CO and O_2 by influencing Fe movement relative to the plane of the porphyrin ring. Inhibition of Fe movement into the heme plane to allow coordination with a sixth ligand appears to be the primary cause of the low affinity observed for the first step in ligand binding to native tetrameric hemoglobin in the T quaternary conformation.[1-4,20] However, this proximal effect does not appear to discriminate greatly between CO and O_2 since the ratio of R to T state affinity constants for both ligands is ~50–100.[7,8] As a result, this review has concentrated on distal interactions between the sixth ligand and surrounding amino acid side chains.

B. The Role of Distal Pocket Amino Acids

Several amino acids in the distal pocket of myoglobin and hemoglobin are highly conserved across species lines, including Phe at position CD1, Val at position E11, Leu at position B10, and most importantly His at position E7 (Figure 2). ValE11 and PheCD1 are in contact with the heme and contribute significant stabilizing hydrophobic interactions that inhibit hemin dissociation.[21,22] The close proximity of HisE7 to the ligand binding site led to the proposal that this residue serves to hinder sterically the binding of CO and thus reduce its affinity for myoglobin and hemoglobin.[15] The crystal structures of model heme compounds with bound CO suggest strongly that the preferred Fe–C–O bonding configuration is linear and perpendicular to the heme plane.[23,24] Distortion from this linear orientation is observed in native sperm whale myoglobin–CO complexes and has been attributed to steric interactions with HisE7.[25] This hindrance was then assigned as the cause of reduced CO affinity in myoglobin. On the other hand, O_2 binds in a bent orientation, and as a result, HisE7 was thought to impose no steric constraint on the Fe–O–O complex. Supporting evidence for the importance of steric hindrance in reducing the CO affinity was provided by ligand binding data on a series of synthetic "picket fence" and "pocket" porphyrins. For the latter compounds, additional steric hindrance near the ligand binding site resulted in unaltered O_2 affinity but decreased CO affinity.[9,15] Until recently, this steric hindrance model has provided the "textbook" explanation for reduced CO affinity in mammalian myoglobins and hemoglobins.[26]

The close proximity of HisE7 to the ligand binding site also allows a hydrogen bond between N_ϵ and the second oxygen atom of the bound ligand. Stabilization of the Fe–O–O complex by H-bonding to the distal histidine was first proposed by Pauling[27] and later confirmed by neutron diffraction studies of the oxymyoglobin complex[28,29] and by spectral studies of cobalt substituted myoglobins and hemoglobins.[30,31] The importance of H-bonding in stabilization of the oxy complex has also been shown for model compounds. For example, O_2 binding to chelated protoheme is enhanced in more polar environments, whereas CO binding appears to be somewhat destabilized.[13,32] In addition, the ligand binding properties of a series of "capped" cyclophane and adamantane model hemes with simple ether or amide linkages also suggest a complex interplay between steric and polar effects.[11,12]

The wealth of structural, biophysical, and biological data available on myoglobin and hemoglobin set the stage to address the questions of molecular recognition of small gaseous ligands by genetic engineering techniques. The development of systems to express sufficient quantities of myoglobins and hemoglobins in heterologous hosts has greatly facilitated determination of the role of specific amino acids in globin function.[33-36] Site-directed mutagenesis combined with detailed structural and biophysical characterizations has allowed quantitative tests of the theories of steric hindrance, hydrogen bonding, and local polarity in regulating ligand binding to myoglobin and hemoglobin. These more recent studies provide the basis for this review. The roles of specific amino acid side chains and their physical effects on ligand binding are discussed below in the context of discrimination between CO and O_2 binding.

A compilation of the ligand binding parameters of selected E7, E11, CD1, CD4, and B10 mutants of myoglobin is given in Table 1. The qualitative agreement between the pig, human, and sperm whale mutants insures the generality of the results.

III. The Binding of Carbon Monoxide

A. Steric Hindrance: Evidence For and Against

1. The Expected Geometry of Fe–C–O in Heme Systems is Linear

A linear Fe–C–O orientation is expected for heme–CO adducts on the basis of orbital overlap in the π back-bonding model of transition metal carbonyl complexes. The crystallographic structure for a CO complex of a pyridine tetraphenylporphyrin confirmed the expected linear Fe–C–O geometry and also indicated that, in the absence of distal steric constraints, the linear Fe–C–O complex is oriented perpendicular to the heme plane.[23,24] More recently, however, Gerothanassis et al.[37] have suggested that the Fe–CO geometry in the unhindered "picket fence" model is actually bent using ^{13}C CP MAS NMR spectra to calculate the ^{13}C shielding tensor (which is a sensitive probe for the Fe–CO orientation). X-ray and neutron diffraction crystal structures of a number of CO-bound myoglobins and hemoglobins reveal CO in variously distorted (tilted and/or bent) conformations.[25,38-42] Despite extensive high-resolution crystallographic data on heme proteins, at present it is not yet possible from structural data alone to determine whether Fe–C–O is linear yet tilted from the heme normal, or whether Fe–C–O is bent with the Fe–C bond perpendicular to the heme plane and the C–O bond off axis. It is clear, however, that there are significant distortions from a linear geometry which is perpendicular to the heme plane. In a recent crystallographic study on the CO geometry in a "capped" porphyrin, the Fe–C–O angle was seen to vary by as much as 7° from linearity, despite the fact there is little or no effect on CO affinity.[43] Other model heme compounds with reduced CO affinity retain a more

Table 1. Rate and Equilibrium Constants for O_2 and CO Binding and Autooxidation Rates for Mb Mutants[a]

protein	k'_{CO} (μM^{-1} s^{-1})	k_{CO} (s^{-1})	K_{CO} (μM^{-1})	k'_{O_2} (μM^{-1} s^{-1})	k_{O_2} (s^{-1})	K_{O_2} (μM^{-1})	K_{CO}/K_{O_2}	k_{ox} (37 °C, h^{-1})	ref(s)
				A. Wild-Type					
sperm whale (SW)	0.51	0.019	27	17	15	1.1	25	0.055	49,52,53,82,111
pig	0.78	0.019	41	17	14	1.2	34	0.07	79,93,111
human	0.76	0.022	35	19	22	0.86	41	ND[b]	112
				B. HisE7 Mutants					
E7Gln(SW)	1.0	0.012	82	24	130	0.180	460	0.021	42,52,112
E7Gly(SW)	5.8	0.038	150	140	1 600	0.090	1 700	44	42,52
E7Gly(human)	4.1	0.041	100	63	1 200	0.053	1 900	ND	112
E7Ala(SW)	4.2	0.061	69	53	2 300	0.023	2 800	58	42,93,111
E7Ala(human)	2.9	0.055	53	46	2 200	0.021	2 500	ND	112
E7Val(SW)	7.0	0.048	150	110	10 000	0.011	14 000	33	42,93,111
E7Val(pig)	6.4	0.050	130	110	14 000	0.0077	17 000	25	74
E7Val(human)	5.4	0.051	100	84	7 700	0.011	9 100	ND	112
E7Thr(SW)	6.9	0.045	150	110	6 400	0.017	8 800	ND	42,93,111
E7Leu(SW)	26	0.024	1 100	98	4 100	0.023	48 000	10	42,93,111
E7Leu(human)	24	0.029	830	120	5 400	0.022	38 000	ND	112
E7Ile(SW)	8.0	0.047	170	90	6 400	0.014	12 000	ND	*c*
E7Ile(human)	5.6	0.044	130	79	11 000	0.0072	18 000	ND	112
E7Met(SW)	4.6	0.023	200	75	1 700	0.045	4 400	>10	52,113
E7Phe(SW)	4.5	0.054	83	75	10 000	0.075	11 000	6	52,93,111
E7Tyr(SW)	0.50	0.092	5.4	6.7	3 200	0.0021	2 600	≥100	22,*c*
E7Trp(SW)	0.65	0.023	28	6.2	87	0.071	390	ND	*c*
E7Arg(SW)	5.7	0.014	400	79	880	0.090	4 400	>10	52,113
E7Asp(SW)	4.4	0.052	85	*d*	*d*	*d*	*d*	>100	52,113
				C. ValE11 Mutants					
E11Ala(SW)	1.2	0.021	56	22	18	1.2	47	0.26	49,93,111
E11Leu(SW)	0.53	0.011	48	23	6.8	3.4	14	0.10	114
E11Ile(SW)	0.050	0.024	2.1	3.2	14	0.22	9.5	0.75	49,93,111
E11Ile(pig)	0.045	0.027	1.7	1.7	14	0.12	14	ND	74
E11Phe(SW)	0.25	0.018	14	1.2	2.5	0.48	29	0.07	49,93,111
E11Ser(SW)	0.28	0.044	6.4	5.1	31	0.16	40	ND	*c*
E11Ser(pig)	1.1	0.044	25	13	35	0.37	68	1.4	74
E11Thr(pig)	0.60	0.080	7.5	2.8	39	0.07	110	3.5	79
E11Asn(SW)	0.041	0.0096	4.3	1.9	0.54	3.5	1.2	ND	50,114,*c*
E11Gln(SW)	0.012	0.011	1.1	0.60	3.4	0.18	6.1	ND	50,114,*c*
				D. PheCD1 Mutants					
CD1Val(SW)[e]	~0.36	~0.050	~7	~16	~100	~0.2	~40	ND	*f*
CD1Trp(SW)	0.23	0.045	5.1	11	63	0.17	30	7.5	*f*
				E. LeuB10 Mutants					
B10Ala(SW)	0.26	0.019	14.0	14.0	18.0	0.80	17	0.24	53,93,111
B10Ala(human)	0.15	ND	ND	4.3	ND	ND	ND	ND	78
B10Val(SW)	0.18	0.016	11.0	8.8	8.3	1.1	10	0.23	53,93,111
B10Ile(SW)	0.23	0.018	13	8.6	10	0.86	15	ND	*c*
B10Ile(human)	0.13	0.020	6.5	5.5	9.0	0.60	11	ND	78
B10Phe(SW)	0.22	0.006	37.0	21.0	1.4	15.0	2.5	0.005	53,93,111
B10Trp(SW)	0.0039	0.008	0.48	0.25	8.5	0.029	16	0.18	*c*
				F. PheCD4 Mutants					
CD4Leu(SW)	0.50	0.056	9.0	13	72	0.18	51	1.5	80
CD4Val(SW)	1.1	0.064	17	14	200	0.069	250	4.9	80

[a] The CO association rate constants were measured both by flash photolysis and stopped-flow rapid mixing techniques. The O_2 association rate constants were measured by laser photolysis techniques. The dissociation rate constants were computed from ligand replacement reactions in which CO was displaced with NO and O_2 was displaced by CO.[110] Equilibrium constants were computed as k'_{O_2}/k_{O_2} and k'_{CO}/k_{CO}. The ligand binding parameters were measured at pH 7.0, 20 °C. The autooxidation rates were measured at pH 7.0, 37 °C, in air-equilibrated buffers. Structures of the proteins marked in ***bold italics*** have been determined by X-ray crystallography and the references are given in the last column. [b] ND, not determined. [c] Li, T.; Singleton, E. W.; Olson, J. S. Unpublished data. [d] The high rate of autooxidation for HisE7Asp precluded the ability to accurately measure O_2 binding parameters. [e] All the kinetic traces for PheCD1Val were biphasic so that the rate parameters are approximate and represent the larger faster phase. [f] Whitaker, T.; Chen, F.; Singleton, E. W.; Li, T.; Olson, J. S. Unpublished data.

linear configuration.[44] Thus, even in cases where atomic resolution is possible, there is no clear relationship between Fe–C–O angle and affinity.

2. Infrared Measurements of the Fe–C–O Angle in Myoglobin

Frauenfelder and co-workers have measured the vibrational frequency of bound C–O at low temperatures.[45] The angle of the CO dipole with respect to the heme normal can be determined by measuring the linear dichroism following photoselective flash photolysis of the Fe–CO complex in the infrared at low temperature. Since the IR transition dipole lies along the CO axis, the angle determined (α) is between CO axis and the heme normal. For native sperm whale myoglobin three different angles are observed, each presumably corresponding to a different conformational substate of CO bound to myoglobin.[45] Room-temperature data on the geometry of bound carbon monoxide also has been obtained by Hochstrasser and co-workers using fast

transient dichroism measurements.[46-48] All methods reveal angles that are off the heme axis with an Fe–C–O angle of approximately 160°.

3. Site-Directed Mutagenesis of Amino Acids E7, E11, CD1, and B10

If steric hindrance were the key factor in regulating CO affinity, then decreasing the size of the amino acid side chains adjacent to the bound ligand should cause marked increases in affinity, whereas increasing the size of the residues should produce the opposite effect. A summary of these studies is presented in Table 1, and the results indicate that steric hindrance does *not* play a dominant role in regulating the CO affinities of the native proteins.

In the case of the E7 mutants, there is little correlation between the number of atoms in the side chain and the CO association equilibrium constant, K_{CO}. Compared to the changes in K_{O_2}, most of the E7 mutants produce only modest 2- to 5-fold changes in CO affinity. The two exceptions are, HisE7Leu which produces a 30-fold increase in K_{CO}, and HisE7Tyr which produces a 6-fold decrease. In the case of E7Tyr metmyoglobin, the phenol side chain chelates directly to the ferric iron atom.[22,49] Assuming a similar conformation in deoxymyoglobin, the proximity of the phenol oxygen to the ligand binding site would be expected to inhibit CO binding, either sterically or electrostatically. However, even for the E7Tyr myoglobin derivative, it is difficult to accept that steric hindrance is the dominant factor since the HisE7Trp mutation has little effect on any of the parameters for CO binding (Table 1). The dramatic increase in K_{CO} observed for the HisE7Leu mutant is not easily explained in terms of relief of steric hindrance by the distal histidine since replacements with physically smaller Gly, Ala, and Val side chains produce much smaller increases in CO affinity. The enhanced CO affinity observed for HisE7Leu remains unexplained despite extensive structural, functional, and spectroscopic characterization.[42,50]

The ligand binding parameters for the E7Arg and E7Asp mutants also seem anomalous since, on the basis of the results for HisE7(native) and E7Gln, polar residues would be expected to show decreased, not increased rates of ligand binding. One possibility is that, as in the case of hemoglobin Zurich β chains which also contain a HisE7Arg mutation,[51] the charged guanidinium group of the E7Arg myoglobin mutant may swing out toward the solvent creating an unhindered, "open" distal pocket.[14] A similar explanation was proposed to explain the high rate of CO binding to the E7Asp mutant, but in this case autooxidation is so rapid that oxygen binding experiments were precluded.[14,52] However, these explanations remain speculative until the crystal structures of HisE7Arg and HisE7Asp myoglobins are determined.

In contrast to the diatomic gases, isocyanide binding does appear to be regulated by the size of residue E7 and serves as paradigm for steric hindrance effects. A roughly linear decrease in $\ln(K_{RNC})$ is observed with an increasing number of atoms in the E7 side chain. As a result, the affinity of E7Phe myoglobin is approximately equal to that for native HisE7 myoglobin for all the isocyanides that have been examined.[52] These results are in marked contrast with those observed for carbon monoxide where there is little difference between the K_{CO} values for mutants containing Gly, Ala, Val, Thr, Ile, Met, and Phe at the E7 position (Table 1).

Initial studies with E11 mutants indicated that the native valine residue does sterically hinder bound CO. Increasing the size of this residue to isoleucine and phenylalanine decreased K_{CO} 15-fold and 2-fold, respectively, whereas decreasing the size to alanine resulted in a 2-fold increase.[49] However, with the exception of the ValE11Ile mutation, these steric effects are small. The importance of polar interactions is quite dramatic when the CO affinities of myoglobins containing valine (native) and leucine at E11 are compared to those of mutants containing threonine and asparagine at this position. In each case, the more polar side chain markedly inhibits CO binding even though the side chains are nearly isosteric (Table 1).

Results for the CD1 mutants also suggest that any steric hindrance on ligand binding provided by this residue is small. Both decreasing the size of this residue by replacement with valine, PheCD1Val, and increasing it, PheCD1Trp, result in decreased CO affinity (Table 1). Similar ambiguity is observed upon replacement of LeuB10. Substitution of LeuB10 with the smaller Ala and Val residues results in 2-fold decreases in CO affinity, whereas increasing the size to Phe actually produces a 30% increase in K_{CO}.[53] (A structural explanation for this result is provided below.) Only when LeuB10 is replaced with Trp is a dramatic decrease in CO affinity observed. A preliminary X-ray structure of the oxy structure of the B10Trp mutant shows that the indole side chain is located directly above the iron atom greatly distorting the Fe–O–O geometry (Li, Olson, and Phillips, unpublished observations).

4. X-ray Crystal Structures of Mutant Myoglobin–CO Complexes

The X-ray crystal structures of CO complexes for wild-type, E7Gly, E7Gln, E7Leu, E11Ala, and E11Phe have been determined[42,50] (Figure 3). Unlike the Kuriyan et al.[25] structure, single CO orientations are observed. In addition, the Fe–C–O is only slightly bent in these structures of recombinant proteins, with angles in the range of 155° to 170°. The most dramatic result is the lack of correlation between Fe–C–O geometry and CO affinity. The bend and tilt angles for the sperm whale myoglobin–CO complexes are all very similar even though their affinities vary greater than 30-fold.[42,50] The C–O angle relative to the heme plane also has been determined using linear dichroism measurements in the IR for sperm whale myoglobin active-site mutants. In all cases the Fe–C–O angle is still off axis, even when the potential steric constraints imposed by active-site residues are removed.[50,54,55] Quantitative comparisons have been presented by Braunstein et al.,[55] Li et al.,[50] Quillin et al.,[42] Li and Spiro,[56] and Ray et al.,[24] and readers are directed to these sources for more information.

In E11Ile myoglobin the C_δ of the isoleucine side chain clearly hinders ligand access to the heme iron atom (Figure 4), and there is a substantial decrease in the affinity of this mutant for carbon monoxide (Table 1). Thus, steric inhibition of CO binding is directly demonstrated, but only in this extreme case, where the

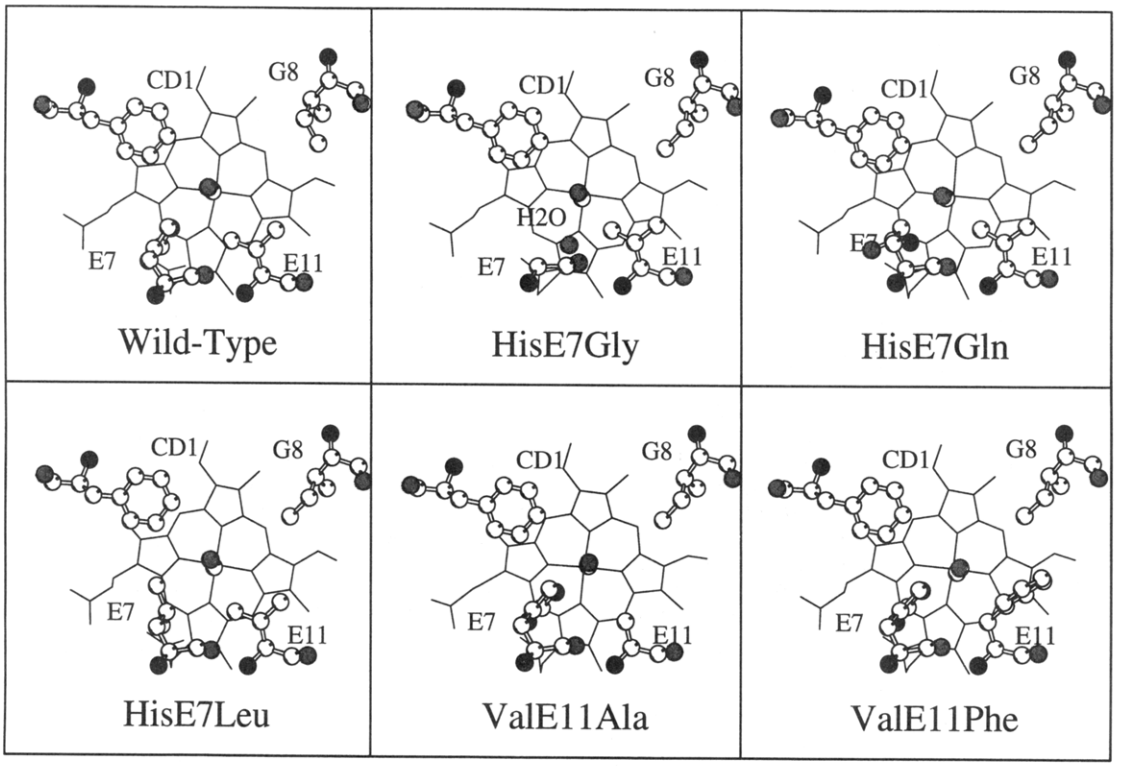

Figure 3. The structures of wild-type and mutant sperm whale myoglobins complexed with CO.[42] The view is from the "top" of the heme and shows selected active-site side chains and heme iron-bound ligand. These structures reveal that the CO ligand for each protein is approximately vertical with only small deviations from linearity. Side chain and ligand carbon atoms are displayed as open circles, nitrogen atoms as closed circles, and oxygen atoms as shaded circles. The top middle panel shows HisE7Gly complexed with CO, and "H2O" defines the positions of a water molecule that resides in a location analogous to the edge of the distal histidine (E7) imidizole in the wild-type structure. The bottom left panel shows HisE7Leu with complexed CO. This mutant has the highest CO affinity thus far discovered, but still has a nonlinear Fe–C–O geometry.

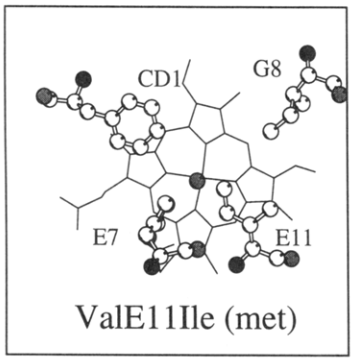

Figure 4. The structure of the met form of the ValE11Ile sperm whale myoglobin mutant.[42] The view is from the "top" of the heme and shows selected active-site side chains and the heme iron-bound water molecule. Side chain and ligand carbon atoms are displayed as open circles, nitrogen atoms as closed circles, and oxygen atoms as shaded circles. This mutant exhibits marked steric constraints on ligand binding due to the C_δ of the isopropyl side chain that overlaps the space just above the heme iron. (The CO structure was not available for this mutant at the time of submission.)

E11Ile side chain is in a position to overlap significantly with the ligand binding site.

B. Electrostatic Interactions in the Distal Pocket

1. Displacement of Distal Pocket Water Molecules

On the basis of the mutagenesis studies presented in Table 1 and Figures 3 and 4, steric hindrance does not appear to be the major determinant of reduced CO affinity in myoglobin. The most likely alternative causes are the requirement to displace distal pocket water molecules and/or direct unfavorable electrostatic effects between the bound ligand and adjacent amino acid residues. Rohlfs et al.[52] have suggested that a major kinetic barrier to O_2 and CO binding involves disruption of hydrogen-bonding interactions between HisE7 and the adjacent water molecule found at ~80% occupancy in the crystal structures of native or wild-type deoxymyoglobins[42] (Figure 5, middle panel). Quillin et al.[42] have proposed that replacement of HisE7 with large apolar residues results in loss of this internal water molecule thus enhancing rates for both CO and O_2 binding (Table 1). Since the Fe–CO complex is relatively apolar, favorable hydrogen-bonding interactions between HisE7 and the bound CO are thought to be weak. As a result, replacement of HisE7 with aliphatic residues should cause increases in K_{CO} by removing the requirement for water displacement. In contrast, the Fe–O–O complex is highly polar and is stabilized by at least −2 kcal/mol through direct hydrogen bonding to N_ϵ to HisE7[14] (Figure 6, upper left panel). Since apolar substitutions at the E7 position prevent this interaction, the net result is a dramatic decrease in O_2 affinity, even though water displacement is no longer required.

This proposed importance of distal pocket water and hydrogen bonding between the bound ligand and HisE7 is supported by the kinetic results in Table 1. Even though the rate-limiting step for CO binding is bond formation with the iron atom, the overall rate constant, k'_{CO}, is proportional to the equilibrium constant for the

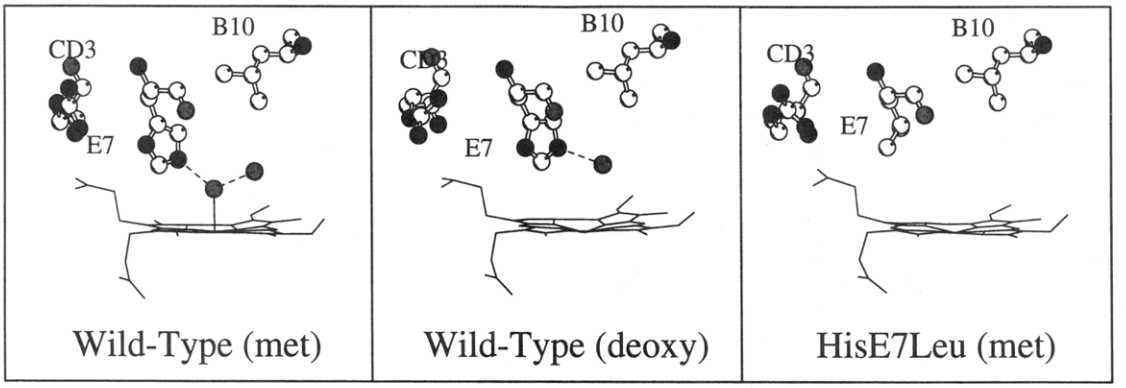

Figure 5. Structures of wild-type sperm whale myoglobin in the met and deoxy states (left and middle panels) and the met form of the sperm whale myoglobin mutant HisE7Leu (right panel).[42] Selected active-site side chains and bound ligand are shown with carbon atoms displayed as open circles, nitrogen atoms as closed circles, and oxygen atoms as shaded circles. Different mutants have different hydration states in the distal pocket. (Left panel) Two water molecules are found in the ligand binding pocket of the met form of myoglobin. One water is covalently bound to the heme iron and another water molecule is found at the rear of the pocket, hydrogen bonded to the first water. (Middle panel) In the deoxy state, wild-type myoglobin has no heme iron covalently bound water molecule, but one remains hydrogen bonded to the HisE7 N_ϵ. This water molecule must be displaced when ligands bind. (Right panel) In comparison, the HisE7Leu mutant myoglobin has a more hydrophobic ligand binding site, i.e.) no covalently bound or hydrogen-bonded water molecules are observed.

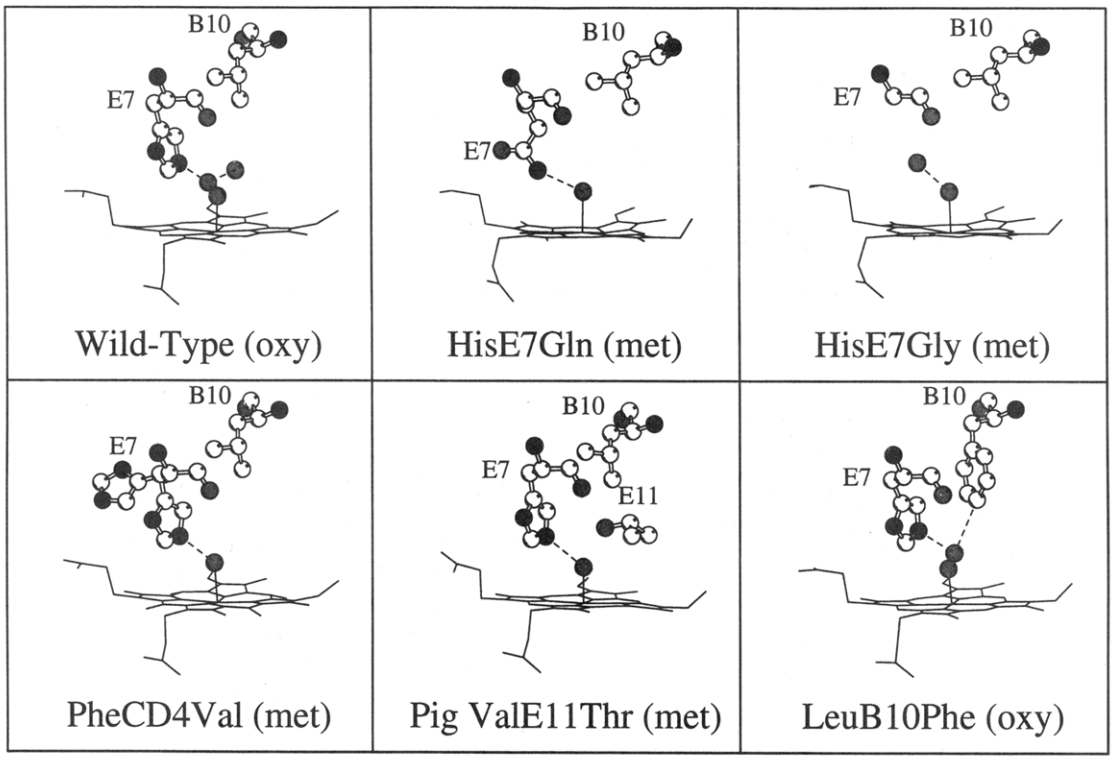

Figure 6. Structures of wild-type and mutant sperm whale myoglobins and a pig myoglobin mutant showing the heme group, bound ligand, and selected active-side chains. Side chains and bound ligand are shown with carbon atoms displayed as open circles, nitrogen atoms as closed circles, and oxygen atoms as shaded circles. Bound oxygen is stabilized by hydrogen bonding. (Top left) O_2 complex of wild-type myoglobin showing a hydrogen bond with the HisE7 N_ϵ and the hydrogen bond network within the distal pocket (dashed lines). A partially bound second water molecule is seen in this form. (Top middle) In the HisE7Gln mutant the Gln side chain can substitute for the HisE7 imidizole and provide a hydrogen bond to heme iron bound water. Of the HisE7 myoglobin mutants thus far examined the HisE7Gln protein has an O_2 affinity and autooxidation rate most like wild-type protein and presumably can donate a hydrogen bond to stabilize bound O_2. Gln at position E7 is found naturally in elephant myoglobin. (Top right) In HisE7Gly myoglobin, a solvent water molecule can partially compensate for the missing imidizole of the HisE7, but there is still a reduction in the oxygen affinity. (Bottom left) The met form of PheCD4Val shows the heme iron-bound water molecule hydrogen bonded to the HisE7 N_ϵ. Two orientations of HisE7 are observed in approximately equal portions. (Bottom middle) The met form of pig mutant myoglobin ValE11Thr showing the heme iron-bound water hydrogen bonded to the HisE7 N_ϵ. (Bottom right) The LeuB10Phe mutant complexed with oxygen showing interactions with the HisE7 N_ϵ and the phenyl ring of B10Phe (dashed lines). This mutant has a remarkably high oxygen affinity due to the dual interaction of the bound dioxygen with the distal histidine and the positively charged edge of the phenyl group of the B10Phe side chain.

noncovalent binding of the ligand within the distal pocket in a location near the final binding site (the "pocket occupancy factor").[57-60] This equilibrium binding process requires the displacement of the distal pocket water molecule found in native deoxymyoglobin and will be enhanced when this water is absent due to

replacement of HisE7 with apolar residues (i.e. E7Leu in Figure 5). Active-site water can also be modulated by solvent perturbation. Carbon monoxide on-rates can be increased 3–4-fold by the addition of a 50% cosolvent (either ethylene glycol and glycerol) which appears to decrease the mole fraction of internal water, thus increasing CO access to the pocket[61] (Chien and Sligar, unpublished observations). This is consistent with cases where the protein provides a semipermeable barrier to cosolvent and ions and loss of interstitial water correlates with osmotic pressure.[62,63]

The overall rate constant for O_2 association, k'_{O_2}, is governed roughly by the rate of movement into the protein and up to the binding site and by the rate of iron–oxygen bond formation. The rate of the former process will be greatly reduced when a water molecule is hydrogen bonded to the distal histidine preventing direct access to the heme iron atom. Thus, regardless of side-chain volume or conformation, polar residues at the E7 position are expected to reduce both k'_{CO} and k'_{O_2}, whereas apolar residues should increase these parameters.

The overall rate constant for CO dissociation, k_{CO}, is determined almost exclusively by the thermal rate of disruption of the Fe–CO bond, whereas k_{O_2} is again governed roughly equally by the rate of Fe–O_2 bond disruption and the rate of escape from the protein.[60] Favorable hydrogen-bonding interactions with the bound ligand should decrease the rate of iron–ligand bond disruption and be manifested as decreases in the overall dissociation constants for either ligand, whereas disruption of these interactions should produce increases in k_{CO} and k_{O_2}. As shown in Table 1, dramatic increases, in some cases up to 1000-fold, are observed for k_{O_2} when HisE7 is replaced with less polar amino acids. These results confirm the importance of hydrogen bonding in stabilizing the Fe–O–O complex. Favorable, but much weaker hydrogen-bonding interactions also appear to occur between HisE7 and bound CO since k_{CO} increases for the same set of mutants, although in this case the changes are ≤4-fold. (See section 3, below.)

2. Structural Evaluation of Distal Pocket Polarity

Quillin et al. have evaluated the water-displacement theory by determining the crystal structures of selected E7 mutants in the aquomet, deoxy, and CO forms.[42] A complete discussion of the role of distal pocket polarity necessitates a description of the ability of H_2O to bind to the ferric form of native and mutant globins. When the heme iron of native or wild-type myoglobin is in the Fe^{3+} state, a H_2O molecule is found coordinated to the iron atom and hydrogen bonded to HisE7 (Figure 5, left panel). Another spherically symmetric peak of electron density is found in the distal pocket of wild-type metmyoglobin and is within hydrogen-bonding distance (2.5 Å) of the coordinated water molecule.[42] This appears to be a second, noncovalently bound water molecule present at ~80% occupancy. Replacement of HisE7 with Leu or Val results in the loss of both water molecules, creating a completely apolar heme pocket, even when the iron atom is in the Fe^{3+} state (Figure 5, right panel).

These crystallographic results confirm previous UV–vis and resonance Raman spectroscopic studies which indicated the absence of coordinated water in the ferric forms of several E7 mutants and abnormal myoglobins and hemoglobins lacking a distal histidine.[64–66] The structure of *Aplysia limacina* metmyoglobin, in which valine occurs naturally at the E7 position, shows no water coordinated to the hemin iron atom.[67] NMR techniques have also indicated the lack of coordinated H_2O in E7Val and E7Phe sperm whale metmyoglobin mutants (G. La Mar, unpublished observations).

In contrast to mutants with large apolar E7 residues, replacement of HisE7 with Gly, Ala, or Gln results in little change in the Soret absorption spectrum of metmyoglobin, indicating that coordinated H_2O is still present in these mutants.[65,66] The sperm whale myoglobin mutant HisE7Thr exhibits a partially blue-shifted Soret maximum, indicating a mixture of penta- and hexacoordinate ferric states.[42] Again, these interpretations were confirmed by crystallography. As shown in Figure 6, coordinated water molecules are found at high occupancy in the crystal structures of E7Gln and E7Gly sperm whale myoglobin. In the glutamine mutant, the water is held in place through a hydrogen bond to the Gln N_ϵ. In the glycine mutant, a second water molecule is found at high occupancy (≥80%) in the position normally occupied by N_ϵ of HisE7 in the wild-type protein and appears to be hydrogen bonded to the coordinated water molecule.

Even though the Fe^{3+}–H_2O bond is broken upon reduction of the heme iron, a well-defined water molecule is still found hydrogen bonded to HisE7 in native and wild-type deoxymyoglobin.[28,42,68] In contrast, no "extra" electron density is found in the distal pockets of the CO forms of any of the myoglobins that have been investigated (viz. Figure 3). These structural data demonstrate that CO binding does result in water displacement and support the idea that this process is a significant kinetic and equilibrium barrier to ligand binding.

3. Polarizability of CO and Hydrogen Bonding

Infrared and resonance Raman studies of the carbon monoxide complexes of a wide variety of heme proteins and model compounds have shown that the stretching frequency of the C–O bond is inversely correlated with that for the Fe–C bond.[50,56,69,70] Li and Spiro have interpreted this inverse correlation between ν_{CO} and ν_{FeC} in terms of back-bond donation from the iron atom.[56] They suggested that proton donors adjacent to the oxygen atom of the bound ligand enhance the degree of back-bonding, increasing the order of the Fe–C bond and decreasing the order of the C–O bond due to the formation of $Fe^{\delta(+)}{=}C{=}O^{\delta(-)}$ resonance structures. The presence of negative electric fields next to the oxygen atom would have the opposite effect, increasing the order of the C–O bond and forming $Fe^{\delta(-)}{-}C{\equiv}O^{\delta(+)}$ resonance structures. Building on this idea, Oldfield and co-workers have proposed that tautomerism of the distal histidine, coupled with movements of the imidazole ring away from the bound ligand can account for the chemical shifts and stretching frequencies of the four observed CO conformers in native myoglobin.[71,72] All of these studies indicate a central role of distal pocket polarity in governing the spectroscopic properties of the bound CO complex.

In order to assess the relative importance of polar versus steric interactions, Li et al. measured the infrared

spectral properties of 41 different recombinant myoglobins containing mutations at HisE7, ValE11, PheCD1, ArgCD3, PheCD4, and LeuB10 positions and correlated these results to the overall CO binding parameters for these same mutant proteins.[50] The results were compared to the crystal structures of CO-bound wild-type, B10Phe, CD4Val, E11Ala, E11Phe, E7Gln, E7Leu, and E7Gly sperm whale myoglobin mutants and of E11Thr pig mutant myoglobin. Vibrational spectra of numerous myoglobin and hemoglobin E7 mutants have been reported.[65,70,73-77] As observed in a number of these previous studies, replacement of the distal histidine (HisE7) with aliphatic amino acids results in a single IR band in the 1960–1970-cm^{-1} region and in large increases in CO affinity (Table 1). More complex behavior was observed for Gly, Ala, Gln, Met, and Trp substitutions at position E7, but in each case there was a net increase in the intensity of this high frequency component. Replacement of ValE11 with Ala, Leu, Ile, and Phe has little effect on the IR spectrum, whereas these mutations result in 20-fold changes in K_{CO}, presumably due to changes in steric constraints. Replacing ValE11 with threonine in pig myoglobin decreases K_{CO} 4–5-fold, whereas the position of the major IR band increases from 1945 to 1961 cm^{-1}. Replacing ValE11 with Asn also results in a large decrease in K_{CO}, but in this case, the peak position of the major IR band decreases from 1945 to 1916 cm^{-1}.[50,73] Nine replacements were made in the CD corner at positions CD1, CD3, and CD4. All of the resultant mutants showed increased stretching frequencies that correlate with movements of the HisE7 imidazole side chain away from the bound ligand.[50,78] All five substitutions at position B10 resulted in altered IR spectra.[50] The LeuB10Phe mutation had the largest effect producing a single band centered at 1932 cm^{-1}.

Together, these and previous data suggest that there is little direct correlation between affinity, ν_{CO}, and Fe–C–O geometry. The major factor governing ν_{CO} appears to be the electrostatic field surrounding the bound ligand and not steric hindrance. The presence of partial positive charges from proton donors, such as N_ϵ of HisE7 and N_δ of AsnE11 cause a decrease in the bond order and stretching frequency of bound CO. In contrast, the negative portion of the ThrE11 dipole points directly toward the bound ligand and increases the C–O bond order and stretching frequency. Movement of HisE7 away from the bound ligand or replacement of this residue with aliphatic amino acids prevents hydrogen-bonding interactions, causing ν_{CO} to increase. Placement of the positive portion of the aromatic multipole from B10Phe next to bound CO causes a decrease in the order of the C–O bond. Substitutions which increase the space available in the distal pocket cause more subtle alterations in the IR spectrum, which can be attributed to increased conformational flexibility and enhanced polar interactions of the bound ligand with solvent water molecules. Thus, the vibrational spectrum of bound CO appears to be a sensitive gauge of electrostatic fields near the ligand binding site in myoglobin. Since there is a strong inverse correlation between ν_{CO} and ν_{FeC}, these IR results indicate that the strength of the Fe–CO bond is governed by electrostatic interactions between the bound ligand and adjacent amino acid side chains. This interpretation is supported by the direct and inverse correlations between the CO dissociation constant, k_{CO}, and the values for ν_{CO} and ν_{FeC}, respectively.[50] Similar correlations have been observed for model heme compounds.[24,56]

4. Electrostatic versus Steric Effects

It is difficult to quantitate the relative importance of direct steric hindrance and electrostatic effects in governing the rate and affinity constants for CO binding to native myoglobin. In some cases discriminating between the two effects is pedantic. For example, Quillin et al. have shown that there is a net displacement of the side chains of either HisE7 or E7Gln out of the distal pocket and toward solvent when CO binds to wild-type myoglobin and the E7Gln mutant.[42] This could be the result of direct steric interactions between the E7 side chain and the bound ligand, or a consequence of displacing distal pocket water molecules which cause the side chains to adopt a more "inward" conformation in deoxymyoglobin. In addition, the noncovalently bound water molecules sterically restrict access to the iron atom, and their presence is a direct consequence of the E7 side-chain polarity.

Despite the ambiguity in interpreting the kinetic parameters for wild-type myoglobin, there can be no doubt about the importance of polar interactions in the distal pocket. The isosteric ValE11Thr mutation in pig myoglobin results in a 5-fold decrease in CO affinity which is due primarily to a 4-fold increase in k_{CO}[79] (Table 1). Since the structures of both the met and CO forms of this mutant are isomorphous with the wild-type structures, these changes must be due to the polarity of the hydroxyl side chain. The E11Thr side chain donates a proton to the carbonyl oxygen of HisE7, and the negative portion of the hydroxyl dipole is pointed toward the bound ligand molecule.[74] The resultant negative electrostatic field stabilizes the $Fe^{\delta(-)}—C\equiv O^{\delta(+)}$ resonance structure weakening the Fe–C bond, decreasing K_{CO}, and increasing k_{CO} significantly (Table 1). Intermediate results were obtained with ValE11Ser mutants.

Positive electrostatic fields adjacent to bound CO (i.e. hydrogen-bonding interactions) should stabilize the $Fe^{\delta(+)}=C=O^{\delta(-)}$ structure, increase K_{CO}, and decrease k_{CO}. Such favorable interactions do appear to occur, but they are small and offset by the concomitant appearance of noncovalently bound distal pocket water molecules in the corresponding deoxymyoglobin derivatives. For example, there may be a weak hydrogen bond between bound CO and HisE7 in native myoglobin due to a small amount of the imidazole tautomer with a proton on the N_ϵ atom[50] (i.e. the small fraction of what is termed the A_3 ground state). Loss of this interaction would account for the increase in k_{CO} observed when HisE7 is replaced with apolar residues. However, the water molecule hydrogen bonded to the distal histidine in native deoxymyoglobin inhibits CO binding to a much greater extent than the small favorable polar interaction stabilizes bound ligand. Similar situations may occur for the E11Asn and E11Gln mutations, but since crystal structures of these mutants have not been determined, this interpretation is speculative.[50]

Further evidence for direct interactions between bound CO and HisE7 comes from work with position

CD4 mutants.[50,80] When PheCD4 is replaced with Val, the imidazole side chain of the distal histidine becomes disordered and appears to be "swinging" between the "up" and "down" conformations shown in Figure 6, bottom left panel. In the CO form of this protein, the HisE7 side chain is predominately in the "up" configuration disrupting any electrostatic interactions with the bound ligand. This results in a 3-fold increase in k_{CO} and a shift in ν_{CO} to higher wave numbers. However, unlike the E7 mutants, the PheCD4Val deoxymyoglobin mutant still contains water molecules, although they are less well-defined and in different positions than those in the wild-type protein. Consequently, there is only a small increase in k'_{CO} and the net result of disordering HisE7 in this mutant is a decrease in CO affinity. Similar results are observed when the HisE7 is protonated at low pH and swings out toward the solvent[42,81,82] (Yang and Phillips, unpublished observations).

IV. The Binding of Oxygen

A. Hydrogen Bonding and the Distal Histidine

1. Previous Ideas and Model Heme Studies

Unlike Fe–CO, the iron–dioxygen complex is highly polar, and bound oxygen is selectively stabilized by hydrogen bonding to HisE7 in almost all myoglobins. The oxy complexes of sperm whale myoglobin and human hemoglobin reveal that the oxygen molecule is bound to the iron atom with a bent, end-on geometry[68,83] as predicted by Pauling.[84] Many authors have argued that the amino acid side chains which compose the ligand binding site are structurally "tailored" to accommodate preferentially the binding of bent O_2[15,68] (Figure 6, top left panel). Similar bent geometries for Fe–O–O were observed in X-ray crystal structures of model heme compound oxy complexes.[85,86] In addition, neutron diffraction studies with native myoglobin and hemoglobin, and spectral studies with cobalt derivatives, have shown that a hydrogen bond occurs between HisE7 and bound oxygen.[28–31] When an inert ether linkage was replaced by an amide proton donor on the ligand binding side of synthetic model "hanging basket" porphyrins, a 10-fold enhanced affinity for O_2 and no effect on CO affinity was observed, confirming the importance of hydrogen bonding interactions.[10,87] The presence of a hydrogen bond between the distal amide proton and the bound O_2 was confirmed by NMR.[88,89] Similar results have been reported for model hemes with distal alcohol or secondary amines[90] and phenylurea substituents.[91]

2. Modulation of O_2 Affinity by Mutagenesis

The oxygen binding parameters for 42 different recombinant myoglobins are presented in Table 1. These data also support the view that the distal pocket residues regulate the binding of diatomic ligands primarily by electrostatic interactions. In deoxymyoglobin, ligand binding is inhibited when polar residues stabilize distal pocket water molecules, whereas in the liganded form proton donors are required to stabilize the polar $Fe^{\delta(+)}–O–O^{\delta(-)}$ complex. The relative magnitude of these two effects governs whether there is an increase or decrease in affinity.

Replacement of HisE7 with any other amino acid results in a substantial decrease in oxygen affinity (Table 1). The reduction in oxygen affinity is the result of large 10–1000-fold increases in k_{O_2} due to the loss of hydrogen bonding between the distal histidine and the bound ligand. The smallest decreases in affinity are observed for the E7Gln, E7Gly, E7Arg, and E7Trp mutants. For the E7Gln mutant, the N_ϵ atom occupies a position similar to that of the corresponding atom in the side chain of HisE7 in the native protein, and thus is in a position to donate a proton to bound O_2. In fact, the HisE7Gln mutation was expected to be relatively conservative since glutamine is found naturally in the E7 position of elephant myoglobin which exhibits similar oxygen and carbon monoxide binding parameters to the sperm whale protein.[92]

The relatively high oxygen affinity observed for the E7Gly mutant was initially more difficult to intepret. However, when the crystal structure of the ferric derivative of this mutant was determined, two intense and spherically symmetric electron density peaks were found in the distal pocket and attributed to water oxygen atoms (Figure 6, top right panel). One water molecule is coordinated to the iron atom, and the second water molecule appears to hydrogen bond to the first and occupies a position almost identical to that of the HisE7 N_ϵ in the wild-type protein (Figure 6, top left panel). If this second water molecule is also present in the oxy structure, it would serve to increase the polarity of the ligand binding site and would help to stabilize bound O_2. A similar situation probably occurs in the distal pocket of E7Arg, but in this case no crystal structure is available for the sperm whale derivative. The causes of the relatively high oxygen affinity of E7Trp and its low dissociation rate constant are less clear.

All of the apolar substitutions result in 3–10-fold increases in k'_{O_2} which are most easily interpreted in terms of destabilization or loss of distal pocket water molecules in deoxymyoglobin. There is little discernible dependence on the size of the side chain. Only in the cases of E7Trp and E7Tyr does steric hindrance appear to play a role in reducing the association rate constant compared to that for wild-type protein. The HisE7Gln mutation produces little change in k'_{O_2} presumably because the polar side chain can also stabilize distal pocket water, although in this case the crystal structure of E7Gln deoxymyoglobin failed to show a single discrete electron density peak attributable to noncovalently bound H_2O.[42]

The importance of the correct orientation of the imidazole ring of the distal histidine is seen in the results for CD1 and CD4 mutants[50,80] (Table 1). The phenyl ring of CD4 places strong constraints on the range of motion of the distal histidine. In the PheCD4Val mutant, multiple orientations of the distal histidine are allowed, and this flexibility would be expected to decrease the strength of the HisE7 hydrogen bond to $Fe–O_2$, accounting for the decrease in O_2 affinity[80] (Figure 6, bottom left panel). Increasing the size of the CD1 residue to Trp also results in decreased oxygen affinity. In this case, the most likely cause is that the indole side chain pushes HisE7 away from the bound ligand, but an exact interpretation will require structural information.

More complex changes occur when ValE11 is mutated, but in general, the results support the view that polar interactions play a more dominant role than direct steric hindrance in governing ligand binding to myoglobin. Removing the γ_2 methyl group by replacing ValE11 with Ala, Leu, and Phe produces no change, a 3-fold increase, and a 2.5-fold decrease, respectively, in oxygen affinity. This suggests that steric hindrance by the naturally occurring ValE11 residue is small. As in the case of CO binding, replacing ValE11 with Ile does cause a 5-fold decrease in affinity due to direct steric hindrance between the bound ligand and the E11Ile C_δ (Figure 4).

Replacing ValE11 with Thr results in a much greater decrease in K_{O_2} than was observed for K_{CO}[79] (Table 1). This reduction in affinity is due both to stabilization of distal pocket water in the deoxy state, which reduces k'_{O_2}, and to electrostatic repulsion between the partial negative charges on the Thr hydroxyl group and bound oxygen, which increases k_{O_2}. Again, intermediate results are observed for the ValE11Ser mutations. The preliminary results for the ValE11Asn and ValE11Gln mutations are remarkable and add further support to the importance of polar interactions in the distal pocket. Both mutations appear to stabilize distal pocket water in the deoxy state and bound oxygen, as seen by the low association and dissociation rate constants for oxygen binding. In the case of the E11Gln mutant, stabilization of distal pocket water and/or steric hindrance by the large E11 side chain appears to dominate, and the net result is a decrease in oxygen affinity. In the case of E11Asn, hydrogen bonding to the bound oxygen appears dominant, causing an increase in K_{O_2}. These interpretations are tentative since the E11Asn and E11Gln mutants have not been characterized crystallographically.

Finally, decreasing the size of residue LeuB10 has little effect on oxygen affinity, however, replacement of this residue with Phe or Trp results in pronounced effects. The LeuB10Phe mutation results in a 15-fold increase in K_{O_2} due primarily to a 10-fold decrease in k_{O_2}. This increase in affinity is a result of direct and favorable electrostatic interactions between the positive edge of the phenyl multipole and the partial negative charge on the second bound oxygen atom[53] (Figure 6, bottom right panel). In the case of B10Trp, the large size of the indole ring sterically hinders the binding of all ligands resulting in ~50-fold decreases in both K_{CO} and K_{O_2}.

3. Interpretation of M Values

The mutagenesis data and structures presented in Table 1 and Figures 3–6 suggest strongly that the ratio, K_{CO}/K_{O_2} or M, is determined primarily by the polarity of the distal pocket. As pointed out by Springer et al., the decrease in M from ~30 000 for simple chelated protohemes in organic solvents to ~30 in mammalian myoglobins is due to an ~100-fold increase in O_2 affinity and a smaller ~10-fold decrease in CO affinity.[14] The increase in K_{O_2} is a result of hydrogen bond formation with HisE7. Although some steric hindrance with distal residues must occur, the decrease in K_{CO} appears to be due primarily to the need to displace the water molecule bound to the same HisE7 residue in deoxymyoglobin. This displacement must also occur in the case of oxygen binding, but is compensated by an even stronger hydrogen-bonding interaction with bound O_2. In the simplest model in which there are no electrostatic interactions with CO, water displacement from the distal histidine results in a 10-fold decrease in both K_{CO} and K_{O_2}, but the hydrogen bond formed with bound oxygen increases the oxygen affinity 1000-fold. The net result is a substantial increase in the selectivity of the protein in favor of oxygen and against carbon monoxide binding.

This interpretation is directly supported by the results for the LeuB10Phe and ValE11Asn mutations. In B10Phe myoglobin, bound O_2 is further stabilized by favorable interactions with the phenyl ring multipole, causing the M value to decrease to 2.5 (Figure 6, bottom right panel). Although speculative, the kinetic results for E11Asn myoglobin suggest that a second hydrogen bond occurs between the asparagine amide nitrogen and bound O_2, causing a further increase in oxygen affinity. The E11Asn residue also appears to stabilize distal pocket water causing a marked decrease in CO affinity. The net result is that E11Asn myoglobin exhibits nearly equal affinities for both O_2 and CO (M = 1.2, Table 1).

V. Heme Iron Autooxidation

In addition to regulating the preferential binding of O_2 over CO, the protein matrix surrounding protoporphyrin IX also serves to prevent autooxidation of the heme iron. Maintaining the Fe^{2+} state is crucial to the function of hemoglobin and myoglobin. In the oxidized state (Fe^{3+}) the heme iron cannot bind O_2 and is physiologically inactive. Free heme in aqueous solution at room temperature autooxidizes within seconds. Once protected by the protein, however, autooxidation slows to hours. Maintenance of the reduced state is also important for protein stability. Hemoglobin and myoglobin have a higher affinity for heme than hemin and the loss of the prosthetic group is the first step in the irreversible denaturation of the protein. In red blood cells and muscle tissue a reductase system helps to keep the proteins reduced.[21]

In the native proteins, and in most mutants still possessing the distal histidine, autooxidation occurs through a combination of two mechanisms.[93] At high [O_2], direct dissociation of the neutral superoxide radical (HO_2) from oxymyoglobin appears to dominate, and this process is accelerated by decreasing pH. At low [O_2], autooxidation occurs by a bimolecular reaction between molecular oxygen and deoxymyoglobin containing a weakly coordinated water molecule. In air-equilibrated buffer at 37 °C, the dominant mechanism appears to be direct, unimolecular dissociation of superoxide from native myoglobin and all of the mutants examined.[93] A summary of autooxidation rates, k_{ox}, under these conditions is presented in Table 1.

The unimolecular HO_2 dissociation mechanism was first proposed by Weiss,[94] championed by Shikama,[95] and is now commonly accepted. The bimolecular reaction mechanism was proposed by Wallace et al.[96] in order to explain the enhancement of autooxidation by anions. Recently, Dickerson et al.[97] have suggested that sterically hindered pentacoordinate model hemes are capable of reacting with O_2 in the absence of a weakly coordinated sixth ligand via an outer-sphere mecha-

Table 2. Rate and Equilibrium Constants for O_2 and CO Binding to Myoglobin and R-State Human Hemoglobin Mutants at pH 7.0, 20 °C

protein	k'_{CO} (μM^{-1} s^{-1})	k_{CO} (s^{-1})	K_{CO} (μM^{-1})	k'_{O_2} (μM^{-1} s^{-1})	k_{O_2} (s^{-1})	K_{O_2} (μM^{-1})	K_{CO}/K_{O_2}
			A. Wild-Type				
Mb(SW)	0.51	0.019	27	17	14	1.1	25
α(Human)	2.9	0.0046	630	28	12	2.3	270
β(Human)	7.1	0.0072	990	110	22	4.5	220
			B. HisE7 Mutants				
Mb(E7Gln)	1.0	0.012	82	24	130	0.180	460
α(E7Gln)	6.5	0.0044	1 500	41	53	0.8	1 900
β(E7Gln)	7.1	0.010	710	91	31	2.9	240
Mb(E7Gly)	5.8	0.038	150	140	1 600	0.090	1 700
α(E7Gly)	19	0.0067	2 800	220	620	0.40	7 000
β(E7Gly)	5.0	0.013	380	100	37	2.7	140
Mb(E7Phe)	4.5	0.054	83	75	10 000	0.007	11 000
β(E7Phe)	5.9	0.014	420	85	43	2.0	210
			C. Val(E11) Mutants				
Mb(E11Ala)	1.2	0.021	56	22	18	1.2	47
α(E11Ala)	32	0.0038	8 400	210	67	3.1	2 700
β(E11Ala)	7.0	0.012	580	180	27	6.7	87
Mb(E11Leu)	0.53	0.011	48	23	6.8	3.4	14
α(E11Leu)	2.5	0.0030	830	24	4.0	6.0	140
β(E11Leu)	6.6	0.011	600	120	20	6.0	100
Mb(E11Ile)	0.050	0.024	2.1	3.2	14	0.22	9.5
α(E11Ile)	0.9	0.0045	200	16	6.8	2.4	83
β(E11Ile)	0.30	0.012	25	12	28	0.43	58
Mb(E11Thr-pig)	0.60	0.080	7.5	2.8	39	0.07	110
β(E11Thr)	7.8	0.016	490	42	18	2.3	210

[a] Rate and equilibrium constants for all the hemoglobin subunits except β ThrE11 were taken from Mathews et al.[99] The rates for β ThrE11 were taken from Fronticelli et al.[102] The ligand binding parameters for the sperm whale myoglobin proteins and references are given in Table 1.

nism; however, the relevance of this mechanism to heme proteins is not yet clear.

The hydrogen bond provided by the neutral imidazole side chain of HisE7 plays the most crucial role in the inhibition of myoglobin heme iron autooxidation. This interaction prevents both dissociation of bound oxygen and its protonation. Replacement of HisE7 with apolar residues results in 100–800-fold increases in the rate of autooxidation due to the loss of this hydrogen bonding interaction (Table 1). In addition, the dependence of k_{ox} on [O_2] for these rapidly oxidizing mutants indicates that the superoxide dissociation pathway is dominant under all conditions. The same relative pH dependence of k_{ox} was observed for native and selected mutant proteins, including some with substitutions at the distal histidine position. This result suggests that protonation of the Fe–O_2 complex accounts for most of the pH dependence observed at or above pH 7.0. Further evidence supporting this idea was obtained using mutations at positions CD3 and E10. Introduction of a negative charge at these positions dramatically increases the rate of autooxidation while introduction of a positive charge inhibits autooxidation.[93] Decreasing the volume of the distal pocket by replacing small amino acids with larger aliphatic or aromatic residues at positions E11 and B10 inhibits autooxidation markedly by decreasing the accessibility of the distal pocket to solvent water molecules, which inhibits protonation of the Fe–O_2 complex (Table 1).

The close mechanistic relationship between autooxidation and oxygen affinity points out the difficulty of constructing stable heme proteins with low oxygen affinities. The hydrogen bond in native myoglobin decreases the rate of autooxidation while raising oxygen affinity. In order to raise the P_{50} of myoglobin, either the hydrogen-bonding interaction should be weakened or steric hindrance of the bound ligand should be enhanced. In single mutants, both these effects cause substantial increases in k_{ox} (i.e. HisE7Gln and ValE11Ile myoglobins). Thus, current attempts to engineer hemoglobin-based blood substitutes with lower affinities for oxygen must take into account the resulting detrimental effects on stability to autooxidation.

VI. Comparison with Hemoglobin

Kinetic parameters are presented in Table 2 for oxygen and carbon monoxide binding to the α and β subunits of R-state human hemoglobin. These constants are defined in terms of the last step in ligand binding to tetramers i.e. $Hb_4X_3 + X \rightleftharpoons Hb_4X_4$. Rate and equilibrium constants for the corresponding myoglobin mutants are included for comparison purposes. More complete discussions of the effects of mutagenesis in hemoglobin have been presented.[98-100] A brief summary is given below.

It appears that the ligand binding site in R-state β subunits can accommodate a variety of nonconservative mutations with little effect on CO and O_2 binding. The HisE7Gly, ValE11Ala, and ValE11Thr mutations result in <2-fold changes in the kinetic and equilibrium parameters for either oxygen or carbon monoxide binding. Thus, the high affinity for O_2 in this subunit must be conferred by some mechanism other than hydrogen bonding to the E7 side chain.[99] Only in the case of the ValE11Ile mutation is a large (10-fold) decrease in O_2 affinity observed, due presumably to direct steric hindrance provided by the β chain E11Ile side chain.

In contrast, R-state α subunits resemble myoglobin on the basis of the effects of mutagenesis. In these subunits, bound O_2 appears to be stabilized by hydrogen

bonding since the HisE7Gly mutation results in an ~5-fold reduction in K_{O_2}. This interaction was predicted by the close proximity of the ϵ-amino nitrogen of HisE7 to the O(2) oxygen atom (2.6 Å in Mb and 2.8 Å in α subunits versus 3.5 Å in β subunits[83]), and this orientation of the bound ligand appears to be fixed by the position of the isopropyl side chain of ValE11. As a result, the favorable hydrogen-bonding interaction is achieved at the expense of increased steric crowding in the distal pocket, limiting access to the ligand binding site. This restriction is manifested as lower association rate constants for all ligands and substantial increases in these kinetic parameters when smaller residues are substituted for HisE7 and ValE11 in R-state α subunits.

The results in Table 2 also show that both hemoglobin subunits discriminate less efficiently against CO binding than myoglobin as manifested by the 10-fold larger M values. The structural origin of this difference is not completely clear. The β-subunit distal pocket appears to be apolar and is little affected by replacing the distal histidine or by replacing ValE11 with threonine. The higher M value for β subunits supports the view that polar interactions play a key role in reducing CO affinity. However, a similar M value is observed for α subunits which do contain a distal pocket water molecule in the deoxy state. In addition, water is coordinated to the ferric iron atoms in both subunits of methemoglobin.

The effects of mutagenesis on T-state ligand-binding parameters are even less well-understood. Only measurements of CO association rate constants, k'_{TCO}, and K_1 or K_T values for O_2 binding have been attempted.[98,100-102] The results indicate that steric and polar interactions in the α-subunit distal pocket are not significantly altered by the R to T quaternary conformational change. This implies that the change in affinity and reactivity of this subunit is due exclusively to changes in proximal HisF8–iron coordination geometry. In contrast, profound changes occur in the β-chain active site as predicted by the crystal structure differences first described by Perutz.[20] The HisE7Gly and HisE11Ala replacements result in 30- and 10-fold increases in k'_{TCO}, whereas the same mutations cause little change in the corresponding R-state rate parameters. This result implies that steric hindrance plays a significant role in reducing ligand affinity in the T state of β subunits. However, more work is needed to evaluate and test these conclusions.

VII. Conclusions

Replacement of highly conserved ligand binding pocket residues by site-directed mutagenesis permits the most direct method of understanding the role of specific amino acids. Comparison of specific amino acid changes from myoglobins and hemoglobins from other species is inevitably complicated by the presence of additional amino acid changes whose influence on the residue of interest is not readily apparent. The correlation between site-specific changes found in naturally occurring mutations, which often give rise to various disease states, has provided relevant information concerning the importance of certain amino acids to protein function and structure.[103] However, in vivo, the strong selective pressure against highly detrimental structural or functional mutations typically precludes the ability to isolate and characterize desired amino acid replacements.

As presented in this review, the ability to couple site-directed mutagenesis with structural and biophysical characterizations has permitted the mechanism of ligand binding discrimination in hemoglobin and myoglobin to be redefined. Although it appears that ligand binding site polarity, water displacement from the E7 residue, and steric constraints are all involved in CO binding, at present it is not possible to quantitate unequivocally the relative contributions of each. It is quite clear, however, that the primary role for the distal histidine in hemoglobin and myoglobin is to provide a stabilizing hydrogen bond to bound oxygen which greatly facilitates the preferential binding of O_2 over CO, and serves to inhibit heme iron autooxidation.

Displacement of water bound to the HisE7 N_ϵ appears to provide a larger barrier to CO binding than does direct steric hindrance by the imidazole side chain. This water-displacement barrier affects both CO and O_2 binding, but the adverse effects on O_2 binding are compensated by the very favorable hydrogen bond provided by the distal histidine. Despite previous claims, the off-axis orientation of CO bound to ferrous myoglobin and hemoglobin is not due to the presence of the distal histidine. Fe–C–O angles $\cong$ 160° have been confirmed independently by X-ray crystallography and low temperature FTIR techniques for most the E7 mutants. It is not yet possible to distinguish between the linear, tilted geometry for the Fe–C–O complex versus the bent geometry, but, again it is apparent that the off-axis orientation is not due to steric hindrance from distal pocket residues. An alternative explanation for the unexpected Fe–C–O geometry might be proximal effects on ligand binding which are more difficult to characterize, or nonplanarity of the iron porphyrin ring in the protein. Precise NMR structures of cyano–met complexes show that some distal pocket mutants exert little effect on the Fe–C–N angle relative to the heme normal, but do markedly reorient and bound ligand in the azimuthal direction.[104,105] Further investigations in this area are clearly required.

The design of heme protein-based blood substitutes is an obvious extension of these studies on the mechanism of ligand binding and inhibition of autooxidation. A number of systems have been developed to produce large quantities of heme-containing protein in heterologous hosts[35,106,107] and efforts in this area are ongoing.[108,109] A sperm whale myoglobin mutant has been engineered with a 10-fold increased O_2 affinity and 10-fold decreased autooxidation rate compared to the native protein.[53] Although this mutant would probably not dissociate O_2 readily enough to be useful in vertebrate tissue, it is clearly a step in the right direction toward the development of a stable extracellular oxygen binding protein capable of substituting for human hemoglobin or serving as a biosensor to monitor O_2 levels. Finally, owing to the diverse chemical reactivities of transition metals, the possibility of rational conversion of myoglobin into an efficient enzyme also has enormous potential in the field of bioremediation.

VIII. Acknowledgments

The authors of this review acknowledge the following support: NIH AR40252 (G.N.P.), GM-35649 and HL-

47020 (J.S.O.), Robert A. Welch Foundation grants C-612 (J.S.O.) and C-1142 (G.N.P.), and the W.M. Keck Foundation.

IX. References

(1) Perutz, M. F. *Annu. Rev. Biochem.* **1979**, *48*, 327–386.
(2) Perutz, M. F.; Fermi, G.; Luisi, B.; Shaanan, B.; Liddington, R. C. *Acc. Chem. Res.* **1987**, *20*, 309–321.
(3) Perutz, M. F. *Annu. Rev. Physiol.* **1990**, *52*, 1–25.
(4) Perutz, M. F. *Trends Biochem. Sci.* **1989**, *14*, 42–44.
(5) Kendrew, J. C.; Dickerson, R. E.; Strandberg, B. E.; Hart, R. G.; Davis, D. R.; Phillips, D. C.; Shore, V. C. *Nature* **1960**, *185*, 422–427.
(6) Perutz, M. F.; Rossman, M. G.; Cullis, A. F.; Muirhead, H.; Will, G.; North, A. C. T. *Nature* **1960**, *185*, 416–422.
(7) Gibson, Q. H. *Biochem. J.* **1959**, *71*, 193.
(8) Antonini, E.; Brunori, M. *Hemoglobin and Myoglobin in Their Reactions with Ligands*; Elsevier Science Publishers B.V.; Amsterdam, 1971.
(9) Collman, J. P.; Brauman, J. I.; Iveson, B. L.; Sessler, J. L.; Morris, R. M.; Gibson, Q. H. *J. Am. Chem. Soc.* **1983**, *105*, 3052–3064.
(10) Lavalette, D.; Tetreau, C.; Mispelter, J.; Momenteau, M.; Lhoste, J.-M. *Eur. J. Biochem.* **1984**, *145*, 555–565.
(11) Traylor, T. G.; Koga, N.; Deardurff, L. A.; Swepston, P. N.; Ibers, J. A. *J. Am. Chem. Soc.* **1984**, *106*, 5132–5143.
(12) Traylor, T. G.; Tsuchiya, S.; Campbell, D.; Mitchell, M.; Stynes, D.; Koga, N. *J. Am. Chem. Soc.* **1985**, *107*, 604–614.
(13) Traylor, T. G.; Koga, N.; Deardurff, L. A. *J. Am. Chem. Soc.* **1985**, *107*, 6504–6510.
(14) Springer, B. A.; Egeberg, K. D.; Sligar, S. G.; Rohlfs, R. J.; Mathews, A. J.; Olson, J. S. *J. Biol. Chem.* **1989**, *264*, 3057–3060.
(15) Collman, J. P.; Brauman, J. I.; Halbert, T. R.; Suslick, K. S. *Proc. Natl. Acad. Sci. U.S.A.* **1976**, *73*, 3333–3337.
(16) Marks, G. S.; Brien, J. F.; Nakatsu, K.; McLaughlin, B. E. *Trends Pharmacol. Sci.* **1991**, *12*, 185–188.
(17) Vandegriff, K. D.; Olson, J. S. *J. Biol. Chem.* **1984**, *259*, 12619–12627.
(18) Lemon, D. D.; Nair, P. K.; Boland, E. J.; Olson, J. S.; Hellmuns, J. D. *J. Appl. Physiol.* **1987**, *62*, 798–806.
(19) Finzel, B. C.; Poulos, T. L.; Kraut, J. *J. Biol. Chem.* **1984**, *259*, 13027–13036.
(20) Perutz, M. F. *Nature* **1970**, *228*, 726–739.
(21) Bunn, H. F.; Forget, B. G. In *Hemoglobin: Molecular, Genetic, and Clinical Aspects*; W. B. Saunders Co.: Philadelphia, PA, 1986; pp 634–662.
(22) Hargrove, M. S.; Singleton, E. W.; Quillin, M. L.; Ortiz, L. A.; Phillips, G. N., Jr.; Olson, J. S.; Mathews, A. J. *J. Biol. Chem.* **1994**, *269*, 4207–4214.
(23) Peng, S.-M.; Ibers, J. A. *J. Am. Chem. Soc.* **1976**, *98*, 8032–8036.
(24) Ray, G. B.; Li, X.-Y.; Ibers, J. A.; Sessler, J. L.; Spiro, T. G. *J. Am. Chem. Soc.* **1994**, in press.
(25) Kuriyan, J.; Wilz, S.; Karplus, M.; Petsko, G. A. *J. Mol. Biol.* **1986**, *192*, 133–154.
(26) Stryer, L. *Biochemistry*; Freeman: New York, 1988; pp 148–150.
(27) Pauling, L. *Nature* **1964**, *203*, 182–183.
(28) Phillips, S. E.; Schoenborn, B. P. *Nature* **1981**, *292*, 81–82.
(29) Hanson, J. C.; Schoenborn, B. P. *J. Mol. Biol.* **1981**, *153*, 117–146.
(30) Yonetani, T.; Yamamoto, H.; Iizuka, T. *J. Biol. Chem.* **1974**, *249*, 2168–2174.
(31) Kitagawa, T.; Ondrias, M. R.; Rousseau, D. L.; Ikeda-Saito, M.; Yonetani, T. *Nature* **1982**, *298*, 869–871.
(32) Suslick, K. S.; Fox, M. M.; Reinert, T. J. *J. Am. Chem. Soc.* **1984**, *106*, 4522–4525.
(33) Nagai, K.; Thogersen, H. C. *Nature* **1984**, *309*, 810–812.
(34) Varadarajan, R.; Szabo, A.; Boxer, S. *Proc. Natl. Acad. Sci. U.S.A.* **1985**, *82*, 5681–5684.
(35) Springer, B. A.; Sligar, S. G. *Proc. Natl. Acad. Sci. U.S.A.* **1987**, *84*, 8961–8965.
(36) Dodson, G.; Hubbard, E.; Oldfield, T. J.; Smerdon, S. J.; Wilkinson, A. J. *Protein Eng.* **1988**, *2*, 233–237.
(37) Gerothanassis, I. P.; Momenteau, M.; Hawkes, G. E.; Barrie, P. J. *J. Am. Chem. Soc.* **1993**, *115*, 9796–9797.
(38) Huber, R.; Epp, O.; Formanek, H. *J. Mol. Biol.* **1970**, *52*, 349–354.
(39) Padlan, E.; Love, W. *J. Biol. Chem.* **1974**, *249*, 4067–4078.
(40) Norvell, J. C.; Nunes, A. C.; Schoenborn, B. P. *Science* **1975**, *190*, 568–569.
(41) Heidner, E. J.; Ladner, R. C.; Perutz, M. F. *J. Mol. Biol.* **1976**, *104*, 707–722.
(42) Quillin, M. L.; Arduini, R. M.; Olson, J. S.; Phillips, G. N., Jr. *J. Mol. Biol.* **1993**, *234*, 140–155.
(43) Kim, K.; Ibers, J. A. *J. Am. Chem. Soc.* **1991**, *113*, 6077–6081.
(44) Kim, K.; Fettinger, J.; Sessler, J. L.; Cyr, M.; Hugdahl, J.; Collman, J. P.; Ibers, J. A. *J. Am. Chem. Soc.* **1989**, *111*, 403–405.
(45) Ormos, P.; Braunstein, D.; Frauenfelder, H.; Hong, M. K.; Lin, S.-L.; Sauke, T. B.; Young, R. D. *Proc. Natl. Acad. Sci. U.S.A.* **1988**, *85*, 8492–8496.
(46) Moore, J. N.; Hansen, P. A.; Hochstrasser, R. M. *Proc. Natl. Acad. Sci. U.S.A.* **1988**, *85*, 5062–5066.
(47) Locke, B.; Lian, T.; Hochstrasser, R. M. *Chem. Phys.* **1991**, *158*, 409–419.
(48) Lian, T.; Locke, B.; Kitagawa, T.; Nagai, M.; Hochstrasser, R. M. *Biochemistry* **1993**, *32*, 5809–5814.
(49) Egeberg, K. D.; Springer, B. A.; Sligar, S. G.; Carver, T. E.; Rohlfs, R. J.; Olson, J. S. *J. Biol. Chem.* **1990**, *265*, 11788–11795.
(50) Li, T.; Quillin, M. L.; Phillips, G. N., Jr.; Olson, J. S. *Biochemistry* **1994**, *33*, 1433–1446.
(51) Tucker, P. W.; Phillips, S. E. V.; Perutz, M. F.; Houtchens, R.; Caughey, W. S. *Proc. Natl. Acad. Sci. U.S.A.* **1978**, *75*, 1076–1080.
(52) Rohlfs, R. J.; Mathews, A. J.; Carver, T. E.; Olson, J. S.; Springer, B. A.; Egeberg, K. D.; Sligar, S. G. *J. Biol. Chem.* **1990**, *265*, 3168–3176.
(53) Carver, T. E.; Brantley, R. E., Jr.; Singleton, E. W.; Arduini, R. M.; Quillin, M. L.; Phillips, G. N., Jr.; Olson, J. S. *J. Biol. Chem.* **1992**, *267*, 14443–14450.
(54) Braunstein, D.; Ansari, A.; Berendzen, J.; Cowen, B. R.; Egeberg, K. D.; Frauenfelder, H.; Hong, M. K.; Ormos, P.; Sauke, T. B.; Scholl, R.; Schulte, A.; Sligar, S. G.; Springer, B. A.; Steinbach, P. J.; Young, R. D. *Proc. Natl. Acad. Sci. U.S.A.* **1988**, *85*, 8497–8501.
(55) Braunstein, D.; Chu, K.; Egeberg, K. D.; Frauenfelder, H.; Morant, J. R.; Ormos, P.; Sligar, S. G.; Springer, B. A.; Young, R. D. *Biophys. J.* **1993**, *65*, 2447–2454.
(56) Li, X.-Y.; Spiro, T. G. *J. Am. Chem. Soc.* **1988**, *110*, 6024–6033.
(57) Doster, W.; Beece, D.; Browne, S. F.; DiIorio, E. E.; Eisenstein, L.; Frauenfelder, H.; Reinisch, L.; Shyamsunder, E.; Winterhalter, K. H.; Yue, K. T. *Biochemistry* **1982**, *21*, 4831–4839.
(58) Gibson, Q. H.; Olson, J. S.; McKinnie, R. E.; Rohlfs, R. J. *J. Biol. Chem.* **1986**, *261*, 10228–10239.
(59) Jongeward, K. A.; Madge, D.; Taube, D. J.; Marsters, J. C.; Traylor, T. G.; Sharma, V. S. *J. Am. Chem. Soc.* **1988**, *110*, 380–387.
(60) Carver, T. E.; Rohlfs, R. J.; Olson, J. S.; Gibson, Q. H.; Blackmore, R. S.; Springer, B. A.; Sligar, S. G. *J. Biol. Chem.* **1990**, *265*, 20007–20020.
(61) McKinnie, R. E.; Olson, J. S. *J. Biol. Chem.* **1981**, *256*, 8928–8932.
(62) Robinson, C. R.; Sligar, S. G. *J. Mol. Biol.* **1993**, *234*, 302–306.
(63) Deprez, E.; Hoa, G. H. B.; Di Primo, C.; Douzou, P.; Sligar, S. G. *J. Biol. Chem.* **1994**, submitted for publication.
(64) Giacometti, G. M.; Brunori, M.; Antonini, E.; DiIorio, E. E.; Wittenhalter, K. H. *J. Biol. Chem.* **1980**, *255*, 6160–6165.
(65) Morikis, D.; Champion, P. M.; Springer, B. A.; Egeberg, K. D.; Sligar, S. G. *J. Biol. Chem.* **1990**, *265*, 12143–12145.
(66) Ikeda-Saito, M.; Hori, H.; Andersson, L. A.; Prince, R. C.; Pickering, I. J.; George, G. N.; Sanders, C. R., II; Lutz, R. S.; McKelvey, E. J.; Mattera, R. *J. Biol. Chem.* **1992**, *267*, 22843–22852.
(67) Bolognesi, M.; Onesti, S.; Gatti, G.; Coda, A.; Ascenzi, P.; Brunori, M. *J. Mol. Biol.* **1989**, *158*, 529–544.
(68) Phillips, S. E. V. *J. Mol. Biol.* **1980**, *142*, 531–554.
(69) Uno, T.; Nishimura, Y.; Tsuboi, M.; Makino, R.; Iizuka, T.; Ishimura, Y. *J. Biol. Chem.* **1987**, *262*, 4549–4556.
(70) Nagai, M.; Yoneyama, Y.; Kitagawa, T. *Biochemistry* **1991**, *30*, 6495–6503.
(71) Oldfield, T. J.; Smerdon, S. J.; Dauter, Z.; Petratos, K.; Wilson, K. S.; Wilkinson, A. J. *Biochemistry* **1992**, *31*, 8732–8739.
(72) Park, K. D.; Guo, K.; Adebodun, F.; Chiu, M. L.; Sligar, S. G.; Oldfield, E. *Biochemistry* **1991**, *30*, 2333–2347.
(73) Balasubramanian, S.; Lambright, D.; Boxer, S. *Proc. Natl. Acad. Sci. U.S.A.* **1993**, *90*, 4718–4722.
(74) Cameron, A. D.; Smerdon, S. J.; Wilkinson, A. J.; Habash, J.; Helliwell, J. R.; Li, T.; Olson, J. S. *Biochemistry* **1993**, *32*, 13061–13070.
(75) Caughey, W. S.; Shimada, H.; Miles, G. C.; Tucker, M. P. *Proc. Natl. Acad. Sci. U.S.A.* **1981**, *78*, 2903–2907.
(76) Morikis, D.; Champion, P. M.; Springer, B. A.; Sligar, S. G. *Biochemistry* **1989**, *28*, 4791–4800.
(77) Sakan, Y.; Ogura, T.; Kitagawa, T.; Fraunfelter, F. A.; Mattera, R.; Ikeda-Saito, M. *Biochemistry* **1993**, *32*, 5815–5824.
(78) Adachi, S.; Sunohara, N.; Ishimori, K.; Morishima, I. *J. Biol. Chem.* **1992**, *267*, 12614–12621.
(79) Smerdon, S. J.; Dodson, G. G.; Wilkinson, A. J.; Gibson, Q. H.; Blackmore, R. S.; Carver, T. E.; Olson, J. S. *Biochemistry* **1991**, *30*, 6252–6260.
(80) Lai, H.-H.; Li, T.; Lyons, D.; Singleton, E. W.; Phillips, G. N., Jr.; Olson, J. S. Manuscript in preparation, 1993.
(81) Tian, W. D.; Sage, J. T.; Champion, P. M. *J. Mol. Biol.* **1993**, *233*, 155–166.
(82) Quillin, M. L.; Brantley, J. R. E.; Johnson, K. S.; Olson, J. S.; Phillips, G. N., Jr. *Biophys. J.* **1992**, *61*, a466.
(83) Shaanan, B. *J. Mol. Biol.* **1993**, *171*, 31–59.
(84) Pauling, L.; Coryell, C. D. *Proc. Natl. Acad. Sci. U.S.A.* **1936**, *22*, 210–216.
(85) Jameson, G. B.; Robinson, W. F.; Collman, J. P.; Sorrell, T. N. *Inorg. Chem.* **1978**, *17*, 858–864.
(86) Jameson, G. B.; Molinaro, F. S.; Ibers, J. A.; Collman, J. P.; Brauman, J. I.; Rose, E.; Suslick, K. S. *J. Am. Chem. Soc.* **1980**, *102*, 3224–3237.
(87) Momenteau, M.; Lavalette, D. *J. Chem. Soc., Chem. Commun.* **1982**, 341–343.

(88) Mispelter, J.; Momenteau, M.; Lavalette, D.; Lhoste, J.-M. *J. Am. Chem. Soc.* **1983**, *105*, 5165–5166.
(89) Gerothanassis, I. P.; Momenteau, M.; Loock, B. *J. Am. Chem. Soc.* **1989**, *111*, 7006–7012.
(90) Chang, C. K.; Ward, B.; Young, R.; Kondylis, M. P. *J. Macromol. Sci. Chem.* **1988**, *A25*, 1307–1326.
(91) Wuenschell, G. E.; Tetreau, C.; Lavalette, D.; Reed, C. A. *J. Am. Chem. Soc.* **1992**, *114*, 3346–3355.
(92) Bartnicki, D. E.; Mizukami, H.; Romero-Herrera, A. E. *J. Biol. Chem.* **1983**, *258*, 1599–1602.
(93) Brantley, R. E., Jr.; Smerdon, S. J.; Wilkinson, A. J.; Singleton, E. W.; Olson, J. S. *J. Biol. Chem.* **1993**, *268*, 6995–7010.
(94) Weiss, J. J. *Nature* **1964**, *202*, 83–84.
(95) Shikama, K. *Biochem. J.* **1984**, *223*, 279–280.
(96) Wallace, W. J.; Houtchens, R. A.; Maxwell, J. C.; Caughey, W. S. *J. Biol. Chem.* **1982**, *257*, 4966–4977.
(97) Dickerson, L. D.; Sauer-Masarwa, A.; Herron, N.; Fendrick, C. M.; Busch, D. H. *J. Am. Chem. Soc.* **1993**, *115*, 3623–3626.
(98) Nagai, K.; Luisi, B.; Shih, D.; Miyazaki, G.; Imai, K.; Poyart, C.; De Young, A.; Kwiatkowsky, L.; Noble, R. W.; Lin, S.-H.; Yu, N.-T. *Nature* **1987**, *329*, 858–860.
(99) Mathews, A. J.; Rohlfs, R. J.; Olson, J. S.; Tame, J.; Renaud, J.-P.; Nagai, K. *J. Biol. Chem.* **1989**, *264*, 16573–16583.
(100) Mathews, A. J.; Olson, J. S.; Renaud, J.-P.; Tame, J.; Nagai, K. *J. Biol. Chem.* **1991**, *266*, 21631–21639.
(101) Tame, J.; Shih, D. T.-B.; Pagnier, J.; Fermi, G.; Nagai, K. *J. Mol. Biol.* **1991**, *218*, 761–767.
(102) Fronticelli, C.; Brinigar, W. S.; Olson, J. S.; Bucci, E.; Gryczynski, Z.; O'Donnell, J. K.; Kowalczyk, J. *Biochemistry* **1993**, *32*, 1235–1242.
(103) Dickerson, R. E.; Geiss, I. *Hemoglobin, Structure, Function, Evolution, and Pathology*; Benjamin Cummings Publishing Company Inc.: Menlo Park, CA, 1983.
(104) Rajarathnam, K.; La Mar, G. N.; Chiu, M.; Sligar, S. G. *J. Am. Chem. Soc.* **1992**, *114*, 9048–9058.
(105) Rajarathnam, K.; Qin, J.; La Mar, G. N.; Chiu, M. L.; Sligar, S. G. *Biochemistry* **1993**, *32*, 5670–5680.
(106) Beck von Bodman, S.; Schuler, M.; Jollie, D.; Sligar, S. G. *Proc. Natl. Acad. Sci. U.S.A.* **1986**, *83*, 9443–9447.
(107) Hoffman, S. J.; Looker, D. L.; Roehrich, J. M.; Cozart, P. E.; Durfee, S. L.; Tedesco, J. L.; Stetler, G. L. *Proc. Natl. Acad. Sci. U.S.A.* **1990**, *87*, 8521–8525.
(108) Looker, D.; Abbott-Brown, D.; Cozart, P.; Durfee, S.; Hoffman, S.; Mathews, A. J.; Miller-Roehrich, J.; Schoemaker, S.; Trimble, S.; Fermi, G.; Komiyama, N. H.; Nagai, K.; Stetler, G. L. *Nature* **1992**, *356*, 258–260.
(109) Hernan, R. A.; Hui, H. L.; Andracki, M. E.; Noble, R. W.; Sligar, S. G.; Walder, J. A.; Walder, R. Y. *Biochemistry* **1992**, *31*, 8619–8628.
(110) Olson, J. S. *Methods Enzymol.* **1981**, *76*, 631–651.
(111) Quillin, M. L.; Brantley, J. R. E.; Johnson, K. A.; Olson, J. S.; Phillips, G. N., Jr. *FASEB J.* **1992**, *6*, 2687.
(112) Dou, Y.; Frauenfelter, F. A.; Ikeda-Saito, M.; Andersson, L. A.; Sakan, Y.; Kitagawa, T.; Pikering, I. J.; George, G. N.; Li, T.; Olson, J. S.; Masuya, F.; Hori, H. Manuscript in Preparation, 1994.
(113) Springer, B. A. Ph.D. Thesis, University of Illinois, Urbana, IL, 1989.
(114) Quillin, M. L.; Li, T.; Olson, J. S.; Phillips, G. N., Jr.; Dou, Y.; Ikeda-Saito, M.; Regan, R.; Gibson, Q. H. Manuscript in preparation, 1994.
(115) Phillips, G. N., Jr.; Arduini, R. M.; Springer, B. A.; Sligar, S. G. *Proteins: Struct., Funct. Genet.* **1990**, *7*, 358–365.
(116) Kraulis, P. J. *J. Appl. Crystallogr.* **1991**, *24*, 946–950.